CONF-910707--2

DE91 015929

FORMATION AND ANNEALING BEHAVIOR OF AN AMORPHOUS LAYER INDUCED BY TIN IMPLANTATION INTO SAPPHIRE

L. J. Romana*, P. S. Sklad, C. W. White, J. C. McCallum*,
A. Choudhury, L. L. Horton and C. J. McHargue*

Oak Ridge National Laboratory
P. O. Box 2008
Oak Ridge, TN. 37831-6118

Phone: 615-574-4344
FAX: 615-574-7659

*L. J. Romana is a post-doctoral fellow with Oak Ridge Associated Universities assigned to Oak Ridge National Laboratory; J. C. McCallum is currently at the Royal Melbourne Institute of Technology, Melbourne, Victoria, Australia; C. J. McHargue is now with The University of Tennessee, Knoxville, TN 37996-2200.

ABSTRACT

The formation and annealing behavior of an amorphous layer produced by tin implantation into sapphire has been studied. Tin ions with 180 keV energy were implanted into α-Al_2O_3 at 300 K with fluences ranging from 10^{15} to 10^{17} ions-cm^{-2}. The thermal stability of the damaged layer was investigated with post-implantation annealing treatments at temperatures up to 1375 K in either oxidizing or reducing atmospheres. The atomic spatial distribution of the ions was determined by Rutherford backscattering spectroscopy (RBS) in random and channeling geometries. The structure of the implanted layer was determined by analytical electron microscopy (AEM). The degree of disorder was found to increase linearly with the fluence up to the threshold for amorphization, ~1 x 10^{16} ions-cm^{-2}. The microstructure of the implanted layer after the thermal treatments depended on the annealing atmosphere. The well-known amorphous $\rightarrow$ γ-Al_2O_3 $\rightarrow$ α-Al_2O_3 phase transition was observed during annealing in a reducing atmosphere. However, anneals in an oxidizing environment led to the formation of the compound SnO_2, which was found to stabilize the cubic γ-Al_2O_3 phase.

INTRODUCTION

During the last few years, there has been increasing interest in the use of ion implantation to modify the mechanical [1-3], electrical [4, 5], and optical properties [6] of ceramics. Relationships between the properties and the structure of the implanted layer have been reported in these investigations. The structure of the implanted layer is, however, difficult to predict because ion implantation involves non-equilibrium processes and because of the complexity of ceramic materials. In the case of sapphire, the amorphization process has been related not only to the amount of deposited energy for the ion implantation

and the irradiation temperature, but also to the nature of the implanted ions [7]. Chemical effects associated with the implanted ions can be illustrated by comparing the amount of deposited energy required for amorphization of sapphire by chromium implantation, 50 keV/atom, and by zirconium implantation, 1.8 keV/atom [8-9]. A preliminary study of tin implantation has also reported sapphire amorphization at low fluence [10].

This paper presents complementary results on the amorphization of sapphire by tin implantation at room temperature. The damage energy level required for amorphization has been determined by Rutherford backscattering spectroscopy (RBS). The charge state of the implanted tin was characterized by X-ray photoemission spectroscopy (XPS). Thermal annealing treatments in a reducing or oxidizing atmosphere have also been carried out in order to study the phase change that occurs when the system attempts to reach an equilibrium state.

EXPERIMENTAL PROCEDURE

High-purity α-Al_2O_3 single crystals with an <0001> surface normal and with an optical grade surface polish were annealed at 1623 K for 120 h in air to remove residual polishing damage and the contamination layer at the surface. The samples were subsequently implanted with 180 keV tin ions using a 200 kV Extrion implanter. An angle of 5º between the surface normal and the incident beam direction was chosen to minimize channeling effects. In order to avoid beam heating, the flux was maintained at $<10^{12}$ ions-cm^{-2}-s^{-1}. The fluences ranged from 1×10^{15} to 1×10^{17} ions-cm^{-2}. The implantations were performed at room temperature. For post-implantation studies, the implanted crystals were

annealed for 1 h at temperatures ranging from 773 to 1373 K in air or in a flowing mixture of 4% H_2 in argon.

The damage induced by ion implantation into the sapphire lattice as well as the implanted ion distribution were characterized by RBS using a 2 MeV He^{++} beam from a Tandem accelerator. RBS in the channeling geometry was performed with the incident beam aligned with the <0001> of the sapphire. The disorder of the aluminum sublattice was characterized by the parameter χ_{Al}, defined as the ratio of aluminum yield (measured at the projected range of the ions) for the aligned spectrum to the yield for the random spectrum. An amorphous layer is claimed when the aligned and random spectra overlap (χ_{Al} =1).

XPS analyses were performed with a V. G. ESCALAB MK II apparatus operating with Mg-k_α radiation.The analysis area was 1000 μm in diameter. The depth profile analysis of the charge state of the implanted ions was studied by sputtering the sample with a 4 keV Ar^+ ion beam. The sputtering rate has been estimated to be about 2 nm-h^{-1} [4].

The microstructure of the implanted layer was characterized by transmission electron microscopy (TEM) of specimens prepared either in cross-section or back-thinned geometries. Analytical electron microscopy (AEM) was conducted with a Philips CM12 instrument operated at 120 keV.

RESULTS AND DISCUSSION

Formation of an amorphous layer

Figure 1 shows the aligned and random RBS spectra obtained from a sapphire substrate implanted at room temperature with 10^{16} ions-cm^{-2}. The aluminum signal for the aligned and random spectra overlapped indicating an amorphous layer with a thickness of ~50 nm. The tin signal is a Gaussian distribution centered at a depth of 45 nm and with a standard deviation of 17 nm. These values are in good agreement with those predicted by TRIM [11] calculations: ion range, $R_{p,}$ = 50 nm and standard deviation, $\Delta R_{p,}$ = 14 nm.

Figure 2 shows the damage buildup in the aluminum sublattice as a function of the deposited energy, F_d, for 180 keV tin implantation as calculated by the E-DEP-1 code [12]. A linear increase of χ_{Al} with F_d is observed up to a value of 0.8 keV/atom, above which an amorphous state is reached. The corresponding fluence is 10^{16} ions-cm^{-2} and the Sn/Al atomic fraction is 0.05. This threshold value for amorphization is very low compared to that for other ion species such as iron [13], for which the threshold value of F_d for amorphization is 7 keV/atom (corresponding fluence of ~10^{17} ions-cm^{-2}), and chromium [9], for which the threshold is 50 keV/atom (6 x 10^{17} ions-cm^{-2}). Therefore, tin implantation induces amorphization of sapphire more easily than does iron or chromium implantations, which suggests that the implanted tin interacts more strongly with the defects produced by elastic collisions and thus suppresses dynamic defect recovery.

Previous TEM analysis performed on a sapphire sample implanted with tin to 4 x 10^{16} ions-cm^{-2} confirmed the presence of an amorphous layer containing clusters which were Sn-rich [10]. Mössbauer results showed that the

tin resides mainly in two charge states, Sn(II) and Sn(IV) [10]. In order to determine the charge state of the implanted tin ions at higher fluences, XPS measurements were performed for a sample implanted with 10^{17} ions-cm^{-2}. The total sputtering depth was about 40 nm. For low tin concentration (i.e., near the surface), only the SnO_2 phase is detected. As the local concentration increases (i.e., approaching the depth of the peak tin concentration), only metallic tin is observed. No metallic aluminum was observed. The different charge states of the implanted tin as a function of the depth from the implanted surface are shown in Fig. 3. Similar evolution of the impurity charge state with the local concentration of implanted ions has been previously reported for sapphire implanted with titanium [4] and niobium [14] .

Annealing behavior of the amorphous layer - Annealing in air

Figure 4 shows the RBS channeling spectra of the aluminum and tin signal after annealing 1 h in air at temperatures of 973, 1233, and 1373 K. An annealing temperature of 1233 K did not modify the observed damage of the aluminum sublattice; however, atomic diffusion of the tin towards the surface was observed. An annealing temperature of 1373 K was required to induce recrystallization of the alumina. After an anneal at 1373 K, the tin distribution was slightly closer to the surface than after the lower temperature anneal. For this annealing temperature, two regions can clearly be identified in the spectrum in Fig. 4a: (1) a well-recrystallized layer is observed between 120 and 50 nm from the surface and (2) a heavily damaged region which extends from the surface to 50 nm. The near-surface region also contains a large fraction of the implanted tin.

In order to identify the microstructure of these different regions, the sample annealed at 1373 K was characterized with TEM. Figure 5 shows a micrograph of a normal plan view of such a specimen. Analysis of the corresponding selected area electron diffraction (SAD) pattern (see the inset in Fig. 5) reveals the presence of γ-Al_2O_3, α-Al_2O_3 and SnO_2. A detailed diffraction analysis reveals that these phases have the following orientation relationship:

$$[0001]\alpha\text{-}Al_2O_3 \,//\, [100]SnO_2 \,//\, [111]\gamma\text{-}Al_2O_3$$

and

$$(30\bar{3}0)\alpha\text{-}Al_2O_3 \,//\, (002)SnO_2 \,//\, (440)\gamma\text{-}Al_2O_3 .$$

From examination of a cross-sectioned specimen, the region between 120 and 50 nm has been identified as α-Al_2O_3 epitaxially aligned with the substrate and the near-surface region has been found to be a two-phase layer composed of SnO_2 and the cubic phase γ-Al_2O_3. The amorphous $\rightarrow$ γ-Al_2O_3 $\rightarrow$ α-Al_2O_3 transition has been reported for stoichiometric implantation of sapphire [15]. However, for stoichiometric implantation of α-Al_2O_3, the cubic phase γ-Al_2O_3 is completely transformed to α-Al_2O_3 at 1373 K. The presence of SnO_2 seems to thermally stabilize the γ-Al_2O_3 phase. Repina et al. [16] have reported that the addition of SnO_2 stabilizes the γ-Al_2O_3 phase and increases the γ-Al_2O_3 $\rightarrow$ α-Al_2O_3 transition temperature.

Annealing behavior of the amorphous layer - Annealing in Ar-4%H_2

Annealing in a reducing atmosphere induced a different recrystallization of the amorphous layer. Figure 6 shows the aluminum and tin RBS signals for a

sample implanted with 4 x 10^{16} ions-cm^{-2} and annealed for 1 h in Ar-4% H_2 at 973, 1233, and 1373 K. After annealing at 973 K, there is no detectable change in the aluminum and tin signals compared to the spectra before annealing. The aligned spectra after annealing at 1233 K indicate that the near-surface region may still be amorphous; deeper in the implanted layer, the substrate has recrystallized. A slight change is observed in the tin signal: the local tin concentration increases, which is probably caused by the precipitation process. TEM micrographs of plan-view specimens reveal that the microstructure of the implanted layer is composed of α-Al_2O_3, γ-Al_2O_3, and a spinel $SnAl_2O_4$ [18]. These phases crystallize with the following orientation relationship:

$$[0001]\alpha\text{-}Al_2O_3 \,//\, [111]SnAl_2O_4 // [111]\gamma\text{-}Al_2O_3$$

and

$$(30\bar{3}0)\alpha\text{-}Al_2O_3 \,//\, (440)SnAl_2O_4 \,//\, (440)\gamma\text{-}Al_2O_3\,.$$

The spectra following a 1373 K anneal show damage recovery throughout the implanted layer. Concomitantly, the spectra indicate that 97% of the implanted tin has diffused from the sample. After annealing at 1373 K, the observation that the aligned spectra for the implanted and virgin regions do not overlap indicates that the residual stress remains in the sapphire lattice.

SUMMARY

Sapphire (c-axis) samples were implanted at 300 K with 180 keV Sn ions to fluences ranging from 10^{15} to 10^{17} ions-cm^{-2}. The threshold fluence for amorphization was found to be 10^{16} ions-cm^{-2}, which is more than one order of magnitude lower than has been reported for iron or chromium implantation.

The thermal stability of the amorphous layer was evaluated with isochronal annealing treatments in reducing and oxidizing environments. In a reducing atmosphere, the implanted layer recrystallizes from an amorphous phase to the γ-Al_2O_3 and then α-Al_2O_3 as the temperature increases from 1233 to 1373 K. After annealing at 1233 K, the γ-Al_2O_3 phase contains $SnAl_2O_4$ precipitates and nearly all of the implanted tin diffuses from the specimen during anneals at 1373 K. In an oxidizing environment, the formation of SnO_2 stabilizes the γ-Al_2O_3 phase which remains up to 1373 K.

ACKNOWLEDGMENTS

The authors would like to thank Drs. P. Thevenard and J. Pawel for helpful technical discussions. Research sponsored by the Division of Materials Sciences of the U.S. Department of Energy under contract DE-AC05-84OR21400 with Martin Marietta Energy Systems, Inc.

References

[1] P. J. Burnet and T. F. Page, J. Mater. Sci., 20 (1985) 4624.

[2] C. J. McHargue, in C. J. McHargue, R. Kossowsky, W. O. Hofer (eds.), Structure-Property Relationships in Surface Modified Ceramics, Vol. 170, NATO ASI Series E, Kluwer Academic Publishers, Dordrecht, 1989, p. 253.

[3] S. M. M. Ramos, B. Canut, L. Gea, P. Thevenard, M. Bauer, Y. Maheo, P. Kapsa, J. L. Lobet, to be published in J. Mater. Res.

[4] L. J. Romana, P. Thevenard, B. Canut, G. Massouras, and R. Brenier, Nucl. Instr. Methods, B46 (1990) 94.

[5] R. Meaudre and A. Perez, Nucl. Instr. Methods, B32 (1988) 75.

[6] M. Treilleux and P. Thevenard, Nucl. Instr. Methods, B7/8 (1985) 601.

[7] C. J. McHargue, G. C. Farlow, G. M. Begun, J. M. Williams, C. W. White, B. R. Appleton, P. S. Sklad, and P. Angelini, Nucl. Instr. Methods, B16 (1986) 212.

[8] C. J. McHargue, P. S. Sklad, P. Angelini, C. W. White, J. C. McCallum, A. Perez, and G. Marest in J. A. Knapp. P. Borgesen, and R. A. Zurh (eds.), Beam-Solid Interactions: Physical Phenomena, Mater. Res. Soc. Symp. Proc. Vol. 157 , Materials Research Society, Pittsburgh, 1990, p. 505.

[9] P. J. Burnet and T. F. Page, J. Mater. Sci., 19 (1984) 845.

[10] C. J. McHargue, P. S. Sklad, J. C. McCallum, C. W. White, A. Perez, E. Abonneau and G. Marest, Nucl. Instr. Methods B46 (1990) 74.

[11] J. F. Ziegler, J. P. Biersack, and U. Littmark, The Stopping and Range of Ions in Solids, Vol. 1, Pergamon Press, New York, 1985.

[12] C. M. Davisson and I. Manning, NRL Report 8859, Naval Research Laboratory, Washington, DC, 1986.

[13] P. S. Sklad, C. J. McHargue, C. W. White, and G. C. Farlow, to be published in J. of Mater. Sci.

[14] S. M. M. Ramos, B. Canut, L. Gea, L. Romana, J. Lebrusq, P. Thevenard, and M. Brunel, to be published in Nucl. Instr. Methods.

[15] C. W. White, L. A. Boatner, P. S. Sklad, C. J. McHargue, J. Rankin, G. C. Farlow, and M. J. Aziz, Nucl. Instr. Methods, B32 (1988) 11.

[16] N. S. Repina, N. F. Ermolenko, and A. A. Prokopovich, Chem. Abst., 76 (1971) Nº 63691.

[17] H. Spandeau and T. Ullrich, Z. Anorg. Chem., 254 (1953) 65.

Figure captions

Figure 1: Random and aligned RBS spectra of unimplanted Al_2O_3 and Al_2O_3 implanted with 180 keV tin ions, 10^{16} ions-cm^{-2}.

Figure 2: Disorder in the aluminum sublattice, χ_{al}, as a function of the deposited energy, F_d, for tin implanted at 180 keV (E-DEP-1 calculation).

Figure 3: Depth evolution of the oxidation state of tin implanted into Al_2O_3 to a fluence of 10^{17} ions-cm^{-2}.

Figure 4: RBS signal of (a) aluminum and (b) tin Al_2O_3 implanted with 180 keV Sn ions to a fluence of 4×10^{16} ions-cm^{-2} and annealed for 1 h in an oxidizing environment at the indicated temperatures

Figure 5: Plan view micrograph of a Al_2O_3 implanted with 4×10^{16} ions-cm^{-2} and annealed at 1373 K in air. The inset shows the corresponding diffraction pattern.

Figure 6: RBS signal for (a) aluminum and (b) tin from Al_2O_3 implanted with 180 keV Sn ions to a fluence of 4×10^{16} ions-cm^{-2} and annealed for 1 h in a reducing environment at the indicated temperatures.

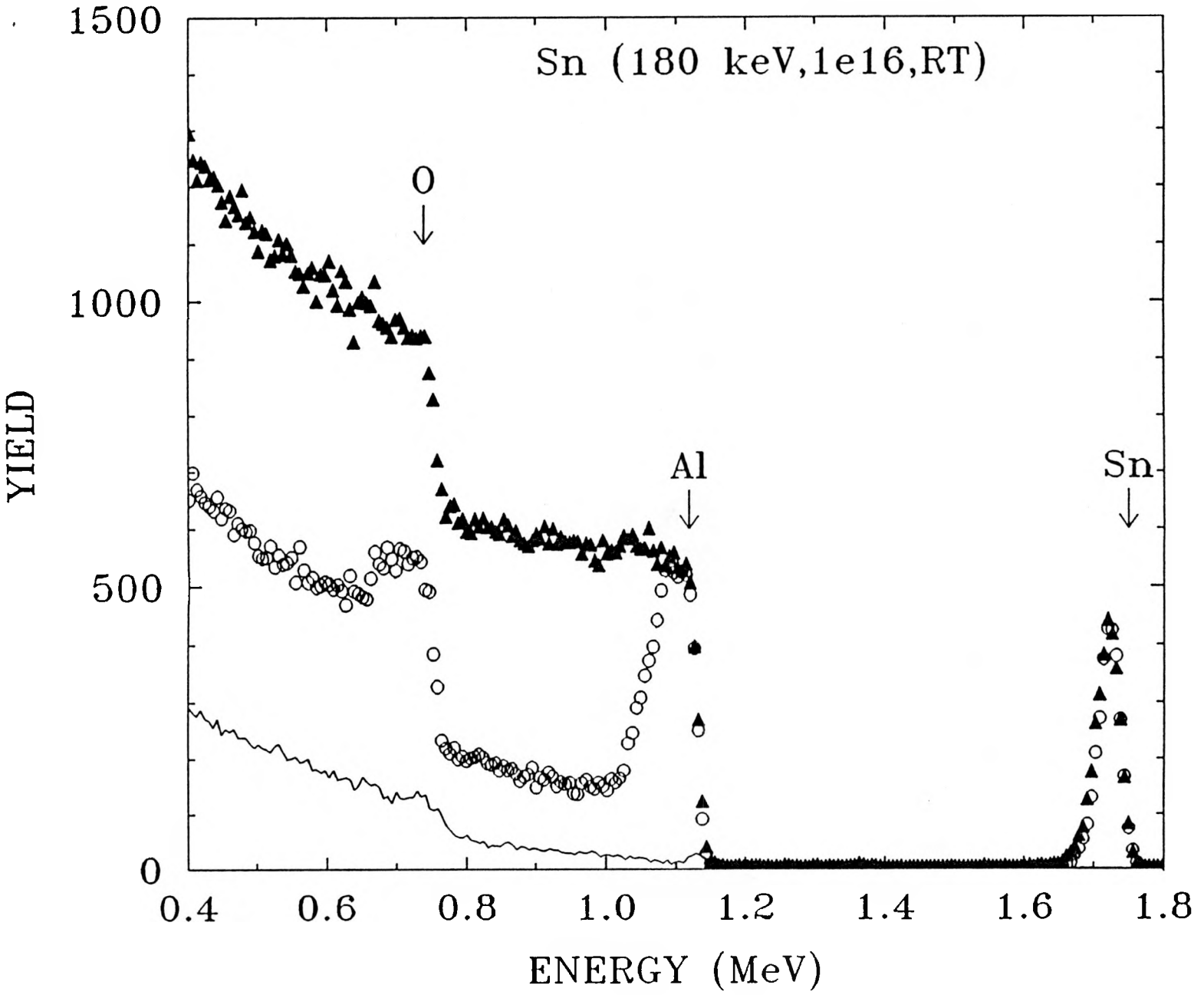
Sn (180 keV,1e16,RT)
O
Al
Sn
YIELD
ENERGY (MeV)
1500
1000
500
0
0.4
0.6
0.8
1.0
1.2
1.4
1.6
1.8

Figure I

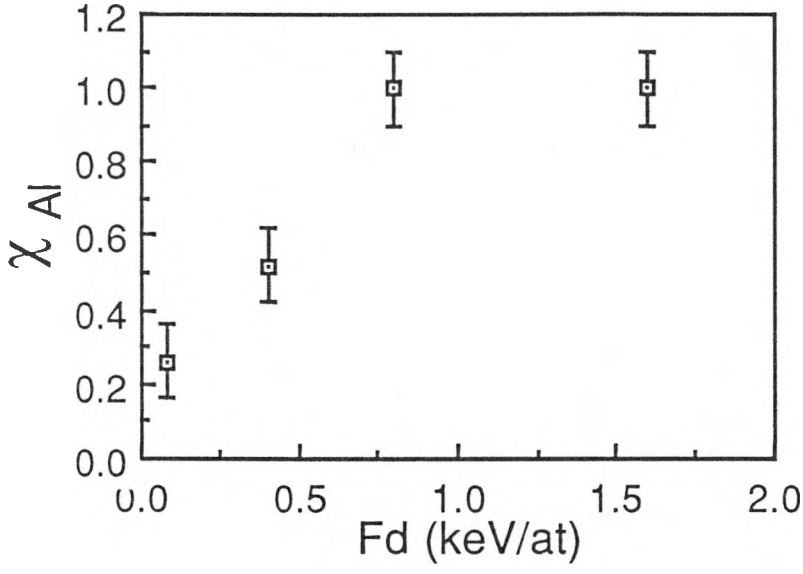
1.2
1.0
0.8
0.6
0.4
0.2
0.0
χ Al
0.0
0.5
1.0
1.5
2.0
Fd (keV/at)

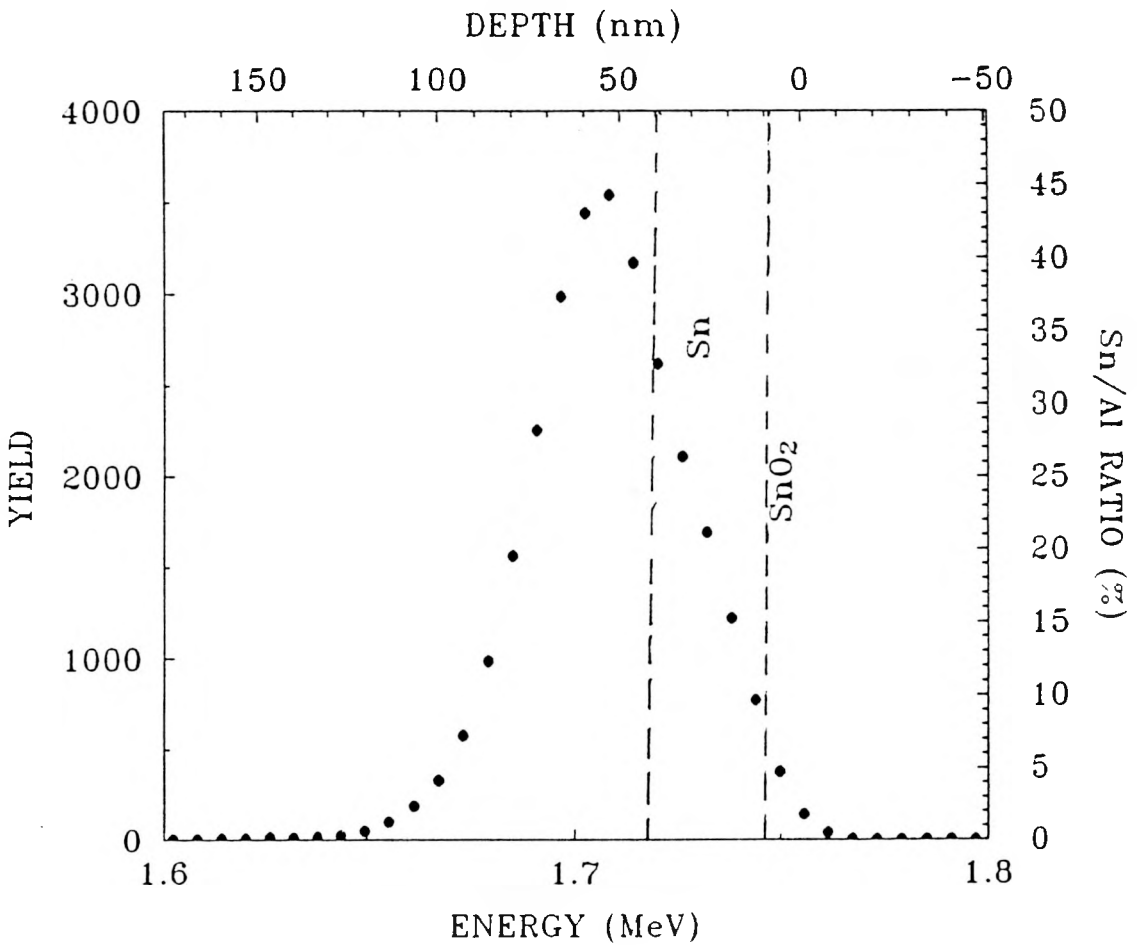
DEPTH (nm)
150
100
50
0
−50
4000
3000
2000
1000
0
YIELD
50
45
40
35
30
25
20
15
10
5
0
Sn/Al RATIO (%)
Sn
SnO2
1.6
1.7
1.8
ENERGY (MeV)

Fig

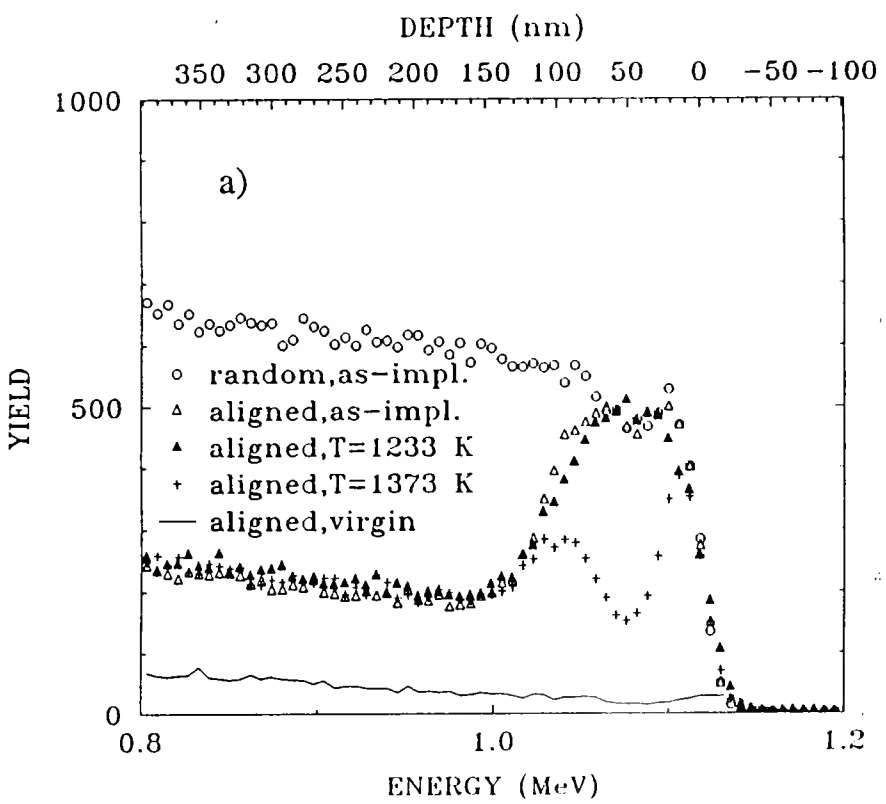
DEPTH (nm)
350 300 250 200 150 100 50 0 -50 -100
1000
500
0
a)
YIELD
random,as-impl.
aligned,as-impl.
aligned,T=1233 K
aligned,T=1373 K
aligned,virgin
0.8
1.0
1.2
ENERGY (MeV)

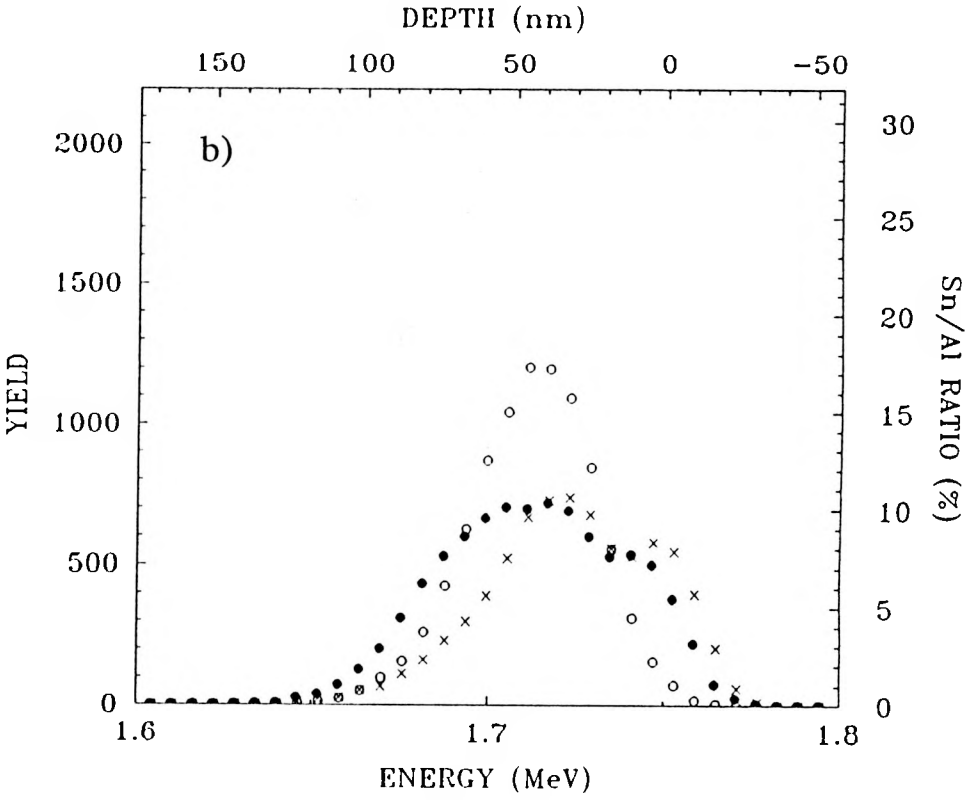
DEPTH (nm)
150 100 50 0 -50
2000
1500
1000
500
0
b)
YIELD
30
25
20
15
10
5
0
Sn/Al RATIO (%)
1.6
1.7
1.8
ENERGY (MeV)

Fig -

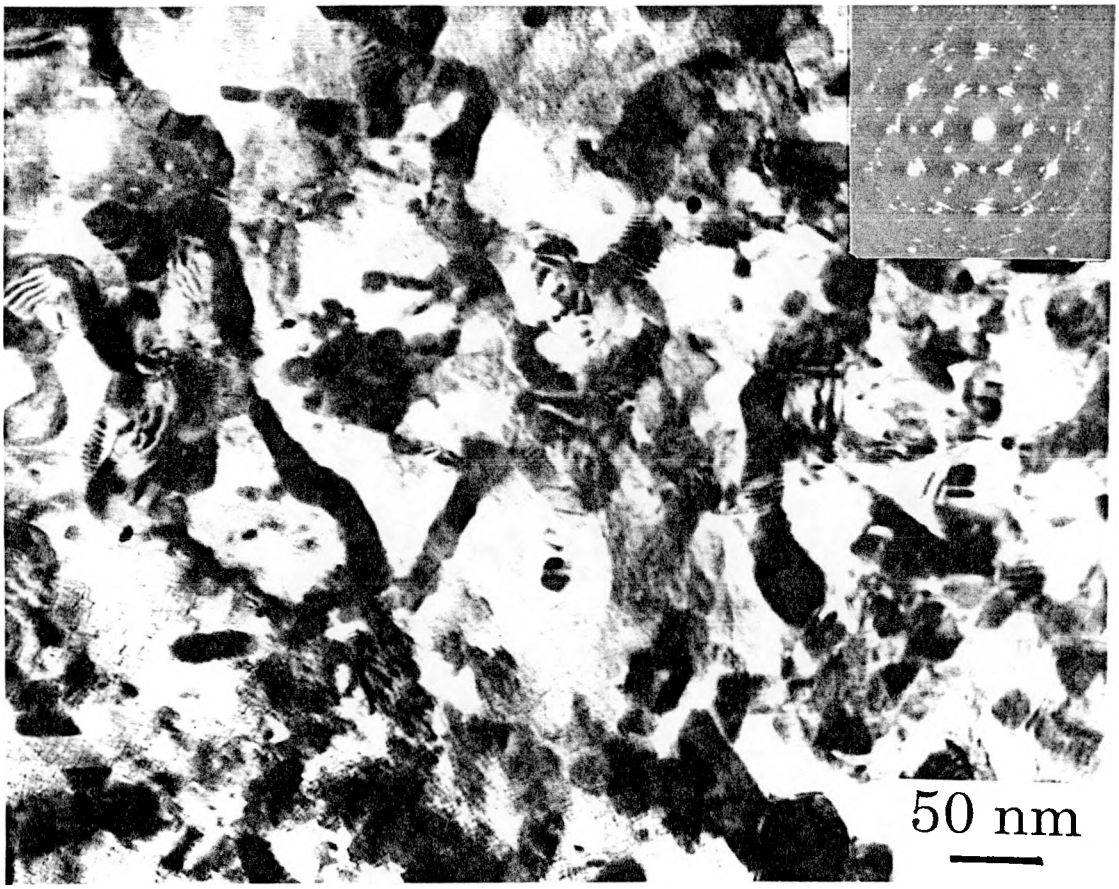
50 nm

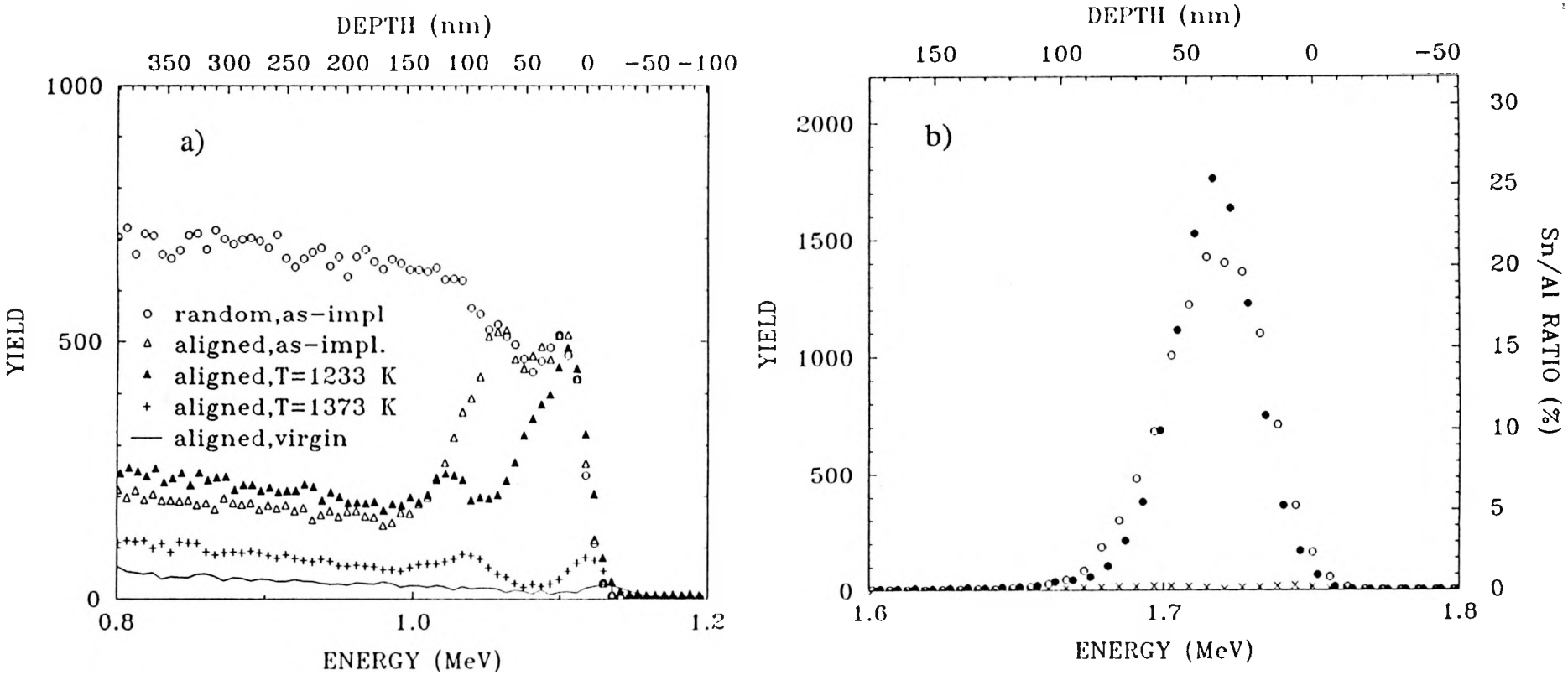
DEPTH (nm)
350 300 250 200 150 100 50 0 −50 −100
1000
500
0
YIELD
a)
random,as−impl
aligned,as−impl.
aligned,T=1233 K
aligned,T=1373 K
aligned,virgin
0.8
1.0
1.2
ENERGY (MeV)
DEPTH (nm)
150 100 50 0 −50
2000
1500
1000
500
0
YIELD
b)
30
25
20
15
10
5
0
Sn/Al RATIO (%)
1.6
1.7
1.8
ENERGY (MeV)

Fig.